FLEXIBLE WIRELESS PASSIVE PRESSURE SENSORS FOR BIOMEDICAL APPLICATONS

Michael A. Fonseca [(1)], Mark G. Allen [(1)], Jason Kroh [(2)] and Jason White [(2)]
(1) School of Electrical and Computer Engineering
Atlanta, GA USA
(2) CardioMEMS, Inc. Atlanta, GA USA

ABSTRACT

Passive resonant sensors have been studied by many groups as an approach to sensing of physical properties in inaccessible locations without the need for incorporating any on-board power sources. In this work, we report two types of **wireless *flexible* micromachined passive pressure sensors**. Since the devices are flexible, they can be rolled or folded into compact shapes suitable for catheter-based delivery into the body. One design is semi-hermetic, intended for acute use. A second design is hermetic, intended for chronic use. Standard flexible and ceramic electronics packaging techniques are used to fabricate the devices. Devices were tested acutely *in vivo* for > 30 days in canine models simulating abdominal aortic aneurysms (AAA) which incorporated a wired reference pressure transducer. The sensor real-time dynamic pressure waveforms were measured and compared to acute devices, with indications for potential extensions to chronic use.

INTRODUCTION

In the measurement of physical parameters within living organisms, passive resonant circuit techniques have been used to create sensors that are wireless, do not require power supplies and can be implanted, both acutely and chronically. Passive resonant circuits used to measure physiological parameters date back to 1957 reported by Mackay [1]. In 1967 Collins reported a miniature "Transensor" ranging in size from 2-6 mm in diameter designed to be implanted in the eye [2]. These devices used two oppositely-wound planar spirals, connected at the periphery, to form an LC circuit with distributed inductance and capacitance. More recently, passive sensors have been developed for continuous measurement of intraocular pressure to monitor glaucoma using two types of sensors: a magnetic sensor and a resonant sensor, reported by [3]. A review of some passive wireless sensing efforts for measurement of physiological parameters was presented in [4]. That work also discussed the development and clinical demonstration in humans of non-flexible passive sensors for monitoring the pressure of abdominal aortic aneurysms (AAA).

Previous work demonstrated a passive wireless scheme used for pressure sensors in high temperature applications [5] and [6]. The concept presented a passive wireless scheme, fabricated from sintered laminated layers of ceramic sheets, indicating use up to 600 ºC. This was achieved through the use of passive resonant circuit structures that were self-packaged and did not incorporate active circuitry or an internal power supply. The fabrication and development began with processing techniques and components from the standard ceramic electronics packaging industry. In a similar lamination-based approach, the work presented in this paper uses standard flex-circuit fabrication techniques to form self-packaged *flexible* wireless passive resonant circuits to measure pressure. Such flexible structures would have the advantage over their non-flexible counterparts that they could be folded into compact shapes during delivery into the body. The devices implement planar spiral inductor coils on flexible polymer film substrates. Similar printed spiral coil structures were developed for transcranial telemetry reported in [7]. Two designs have been studied: a semi-hermetic design using liquid crystal polymers which has high ease of fabrication and is suitable for acute use; and a hermetic design using ceramic-encapsulated pressure references intended for chronic use.

DESIGN AND FABRICATION

The sensors in this work consist of a cavity, bounded on two sides by capacitor plates or distributed capacitive structures, resonantly interconnected with an inductance. If either the top or bottom (or both) sides of the cavity are made of a deflectable diaphragm, the value of this capacitor will change with pressure. The resultant pressure-induced change in the resonant frequency of the distributed passive LC circuit can be measured wirelessly using an external magnetic loop.

Standard flexible electronic packaging techniques are used to fabricate the sensors. Sensors designed for acute use are fabricated from laminated sheets of copper-clad Liquid Crystal Polymer (LCP) and expanded polytetrafluoroethylene (PTFE)-based inner bonding layers. The copper cladding is patterned into the desired inductor structures prior to lamination through standard lithography and wet-chemical etching. This approach results in a self-packaged structure in which only a polymer outer surface is exposed to the environment. The inductor coil layout uses a planar spiral inductor with 12 turns, line width of 60 micron, line spacing of 80 micron, and line thickness of 18 micron; the starting radius for the spiral inductor is 3.8mm. The capacitor plate area for the LCP sensor design is 13.1mm^2. *Figure 1 (a)* illustrates the planar coil design for the LCP design.

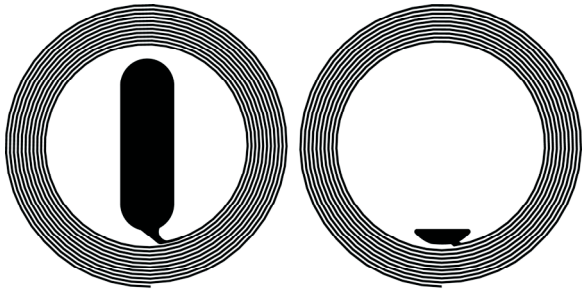

Figure 1 *Planar spiral inductor layout for (a) LCP sensor design and (b) PTFE/ceramic chamber design.*

The inner layer of the LCP sensor, illustrated in *Figure 2 (a)*, is laser-cut using an excimer laser (248 nm wavelength) to achieve accurate dimensions. The span was designed to be 2mm at the ends and 1.4mm at the center with a length of 6.68mm. The cavity was tapered in the center to reduce the deflection and avoid shorting out the capacitor over pressure excursions of interest.

0-9640024-6-9/hh2006/$20©2006TRF
DOI 10.31438/trf.hh2006.9

Solid-State Sensors, Actuators, and Microsystems Workshop
Hilton Head Island, South Carolina, June 4-8, 2006

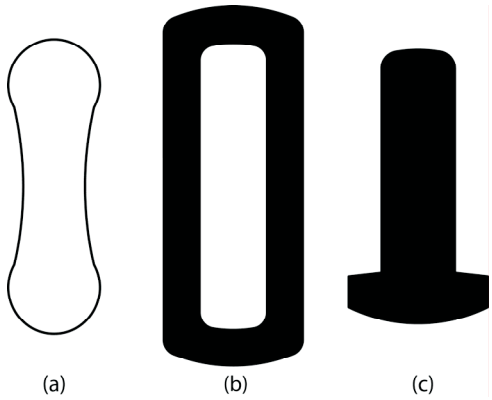

Figure 2 *Inner layer designs for (a) the LCP sensor, (b) ceramic chamber and (c) electrode on the ceramic chamber.*

The layers are aligned via registration pins on platens, assembled and laminated at 180 ºC for 80 minutes with 431 kPa of pressure, illustrated in *Figure 3*. The batch process uses 4 inch sheets with 4 rows and 4 columns, yielding 16 devices per fabrication run. The sensors are individualized using the same excimer laser to achieve various shapes for minimally-invasive delivery. A fabricated sensor is illustrated in *Figure 5 (a)*.

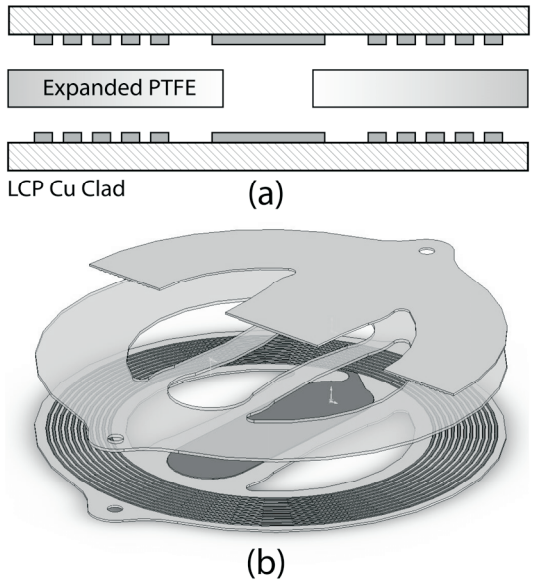

Figure 3 *Sensor lay up for acute use. (a) Cross-sectional view and (b) perspective view of the LCP sensor design.*

Sensors designed for chronic use are fabricated from both copper-clad and non-clad PTFE layers, Fluorinated Ethylene Propylene copolymer (FEP) inner layers, and an encapsulated ceramic chamber (housing the hermetic pressure reference), again resulting in self-packaged structures. Only a PTFE outer surface is exposed to the environment.

The planar inductor coil layout for the PTFE sensor design, illustrated in *Figure 1 (b)*, has the same physical dimensions as the LCP design described above. The chambers are fabricated through the used of sintered layers of zirconia ceramic powders using a standard green-tape approach [6]. The layout design has spans ranging from 1.7- 2.5mm and gaps from 25-50 microns, illustrated in *Figure 2 (b)* and *Figure 4*. The inner layer of the chamber is laser-cut in a green state using a Nd:YLF infrared laser (1 micron wavelength). The sheets are aligned and assembled, three sheets per stack, with thicknesses between 25-35 microns, laminated in a press, and sintered in a box furnace at temperatures between 1300-1500 °C. The ceramic chambers are batch-fabricated with 54 chambers per sheet on a 4 inch sheet. After the ceramic chambers are sintered, they are individualized for assembly into each polymer sensor.

The PTFE and FEP inner layers are laser cut using a CO_2 (10.6 micron wavelength) laser for the solder connection, illustrated in *Figure 4 (a)*, and chamber assembly. The copper clad, inner PTFE and FEP layers, ceramic chambers and solder pellets are aligned and assembled (16 devices per run on 4 inch sheets). The sheets are vacuum laminated in a hot press at 300 °C, for 60 minutes with 431 kPa of pressure. The vacuum eliminates trapped gas between the FEP and ceramic chamber. The sensors are individualized using a CO_2 laser to achieve various shapes for minimally-invasive delivery. A fabricated sensor is illustrated in *Figure 5 (b)*.

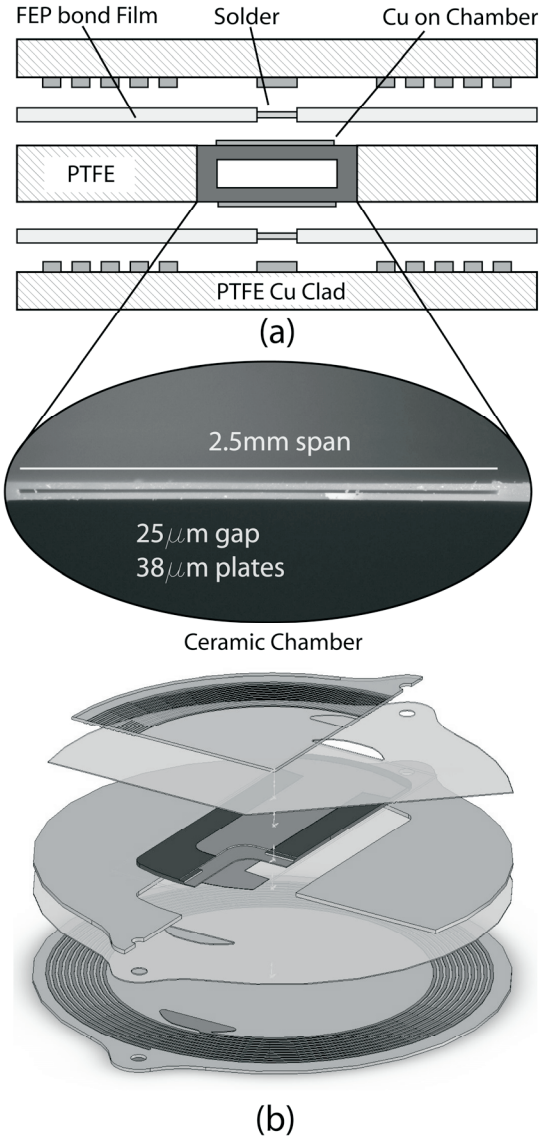

Figure 4 *Sensor lay up for chronic use. (a) Cross-sectional view and (b) perspective view for the PTFE/Ceramic chamber sensor design.*

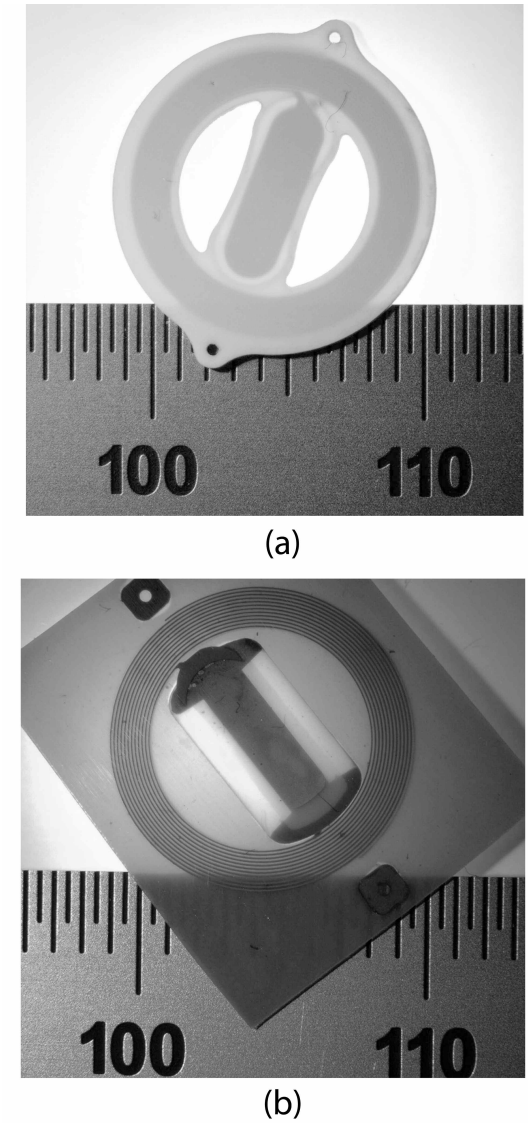

Figure 5 *Fabricated for (a) acute use using LCP polymer and (b) chronic use using PTFE with ceramic pressure sensitive chamber.*

THEORY AND DEVICE CHARACTERIZATOIN

The development of a circuit model was reported in previous work for passive LC resonant circuits [5] and [6]. The sensors described above can be modeled by a lumped LCR circuit, illustrated in *Figure 6*. Analysis of the circuit results in the input impedance referenced to the terminals of the coupling coil. Substituting into the input impedance $f_o=[2\pi(LC)^{½}]^{-1}$, $k=L_m(L_aL_s)^{-½}$ and $Q=\omega L_sR_s^{-1}$ results in Eq. 1 below.

$$Z_1 = \frac{V_1}{I_1} = j2\pi f L_a \left[1 + k^2 \frac{\left(\frac{f}{f_o}\right)^2}{1-\left(\frac{f}{f_o}\right)^2 + \frac{1}{Q} j \frac{f}{f_o}} \right] \qquad (1)$$

Eq. (1) can be used to fit impedance measurements from a network analyzer and pickup-coil in order to extract the resonance frequency and quality factor, illustrated in *Figure 7*.

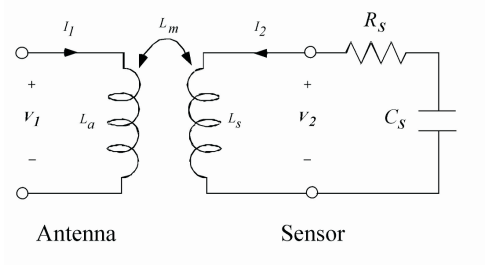

Figure 6 *Equivalent circuit of electrical model for a sensor coupled with an antenna.*

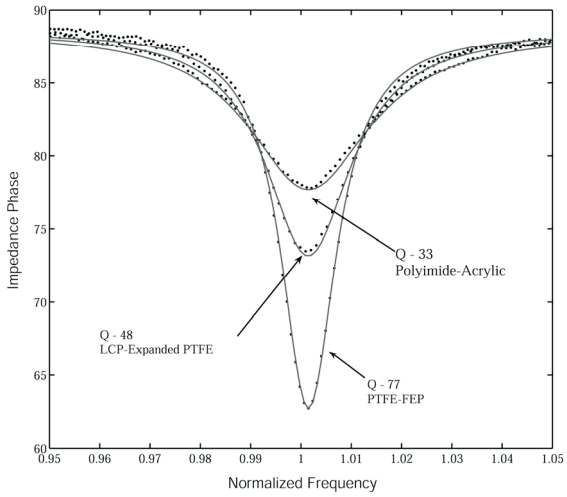

Figure 7 *Impedance Phase data (dots) and model curve fit (line) vs. normalized frequency for three different substrates*

Throughout the development of the two sensors described above, various flexible substrates were tested and characterized. These include polyimide-acrylic, LCP/expanded PTFE, PTFE, PTFE/FEP, and PTFE/FEP/Ceramic. For each progression of substrate material, increasing values of quality factor were achieved; similarly different values of hermeticity were achieved. In order to compare substrates, the layout for the planar spiral inductors were limited to those in *Figure 1*, resulting in resonant frequencies ranging from 30-50 MHz. *Table 1* below lists quality factors achieved vs. substrate materials and electrical characteristics.

Table 1 *Quality factors achieved vs. substrate material and electrical characteristics*

Substrate/Bonding Film	Quality Factors	Dielectric Constant @ ≥ 1 MHz	Dielectric Loss @ ≥ 1 MHz
Polyimide-Acrylic	25-35	(3.7)/(3.6)	(0.0014)/(0.035)
LCP/expanded PTFE	45-55	(2.9)/(2.6)	(0.0025)/(0.004)
PTFE	55-65	2.2	0.0008
PTFE/FEP	65-77	(2.2)/(2.05)	(0.0008)/(0.0006)
PTFE/FEP/Zirconia	60-65	(2.2)/(2.05)/(29)	(0.0008)/(0.0006)/(0.001)

The linear pressure sensitivity of several devices was characterized between -1 to -20 kHz/mmHg for LCP/expanded PTFE devices and -0.5 to -1.5 kHz/mmHg for PTFE/FEP/Ceramic devices. The difference in sensitivities is attributed in part to the increased modulus of the ceramic layer of the pressure sensitive membrane.

The electrical properties were characterized in both deionized (DI) water and saline solution in order to simulate *in vivo* conditions. In both designs, the DI water environment resulted in frequencies lower than those measured in air. In the saline

environment, the measurements resulted in a lowering of quality factor as well as frequency compared to measurements in air. When submerged in saline, both device designs dropped in frequency by ≥ 3 MHz and dropped in quality factor to ≤ 40. These initial changes were followed on the LCP/expanded PTFE design by a gradual decrease in frequency over a timeframe of several days. The PTFE with ceramic pressure sensitive chamber devices showed only the immediate changes, with no significant gradual change.

The initial frequency upon immersion in saline or DI water was attributed to the change in dielectric constant of the surrounding environment (shift from air ε_r ~1 to saline ε_r ~80). The increase in dielectric constant increased parallel paths of electric field through the surrounding media, increasing the total capacitance of the system, leading to a decrease in resonant frequency.

The decrease in quality factor in saline was attributed to the change in loss tangent between air or DI water to saline (from approximately 0 to 0.2); penetration of electromagnetic field lines into this high loss tangent environment increases total losses and reduces the quality factor.

In order to reduce the offsets, losses, and potential drift due to changes in the dielectric environment in which the sensors are embedded, the devices were coated with approximately 0.3 mm thick outer layer of silicone. The addition of this low dielectric constant and low-loss insulating material reduced the fringe electric fields exiting into the surrounding media and reduced this effect. Typical shifts in frequency after silicone coating were < 0.7 MHz, with quality factors dropping between 3-5 points. These offsets could be reduced further for these designs by coating to a greater thickness. Catheter based delivery of the devices limited the total thickness of the sensors.

For LCP based devices, the average normalized frequency drift in saline (under zero applied pressure) was measured to be ≤ -1.75 ±0.32 %, reaching stability after 250 hrs. This is equivalent to -0.612 MHz for a 35 MHz device, and equates to a pressure-equivalent baseline drift of 61.2 mmHg for devices with nominal pressure sensitivities of -10 kHz/mmHg. This baseline drift could be attributed to many factors including moisture absorption into the polymer and/or into the reference pressure chamber of the sensor. For PTFE-ceramic based devices the average normalized frequency drift in saline (under zero applied pressure) was measured < ±0.002% for over 20 hours. This is equivalent to ≤ ±0.7 kHz for a 35 MHz device, and equates to a pressure-equivalent baseline drift of less than 1 mmHg at a nominal pressure sensitivity of 1 kHz/mmHg.

IN VIVO EXPERIMENTAL RESULTS

The devices were tested *in vivo* in canine models simulating abdominal aortic aneurysms, illustrated in *Figure 8*, with LCP based acute devices that were implanted and measured. The aneurysms were created by surgically implanting a graft and wired reference pressure transducer into the aorta. The canine model is described in greater detail in [8]-[10]. After the animal was allowed to heal, the sensors were implanted through catheter delivery, following which a stent graft was used to perform endovascular repair. The following section will describe the catheter and electronics used throughout the test along with measured results.

CATHETER DELIVERABILITY

For minimally invasive implantable devices, catheter based delivery systems are preferable. The flexible sensors could be rolled or folded into catheters that have internal diameters of ≤ 4 mm. The delivery system used for this study consisted of a delivery catheter, sheath, deployment-clip and sensor-tether, illustrated in *Figure 9 (a)*. The sensor is attached to a small diameter (0.020" OD) 'tether tube', *Figure 9 (b)*, by threading a small diameter (0.008") nitinol wire through the length of the tube, and through holes on the top and bottom portion of the sensor, which are shown in *Figure 5 (a)*. The tether tube maintains control over device position in the aneurysm sac by the user, until completion of the endovascular repair with the stent graft. At the time of release, the thin wire is pulled by the user to release the sensor in the desired location within the aneurysm.

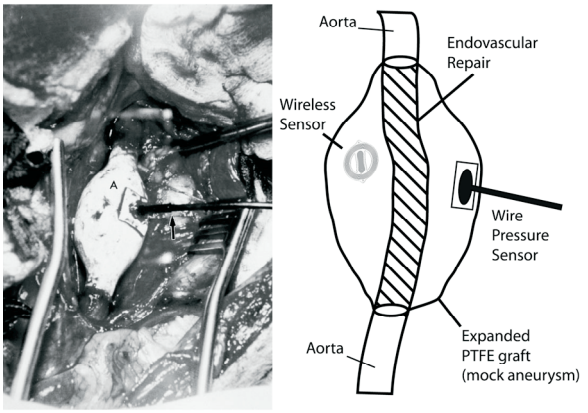

Figure 8 *Creation of mock aneurysm and position of wired and wireless sensor*

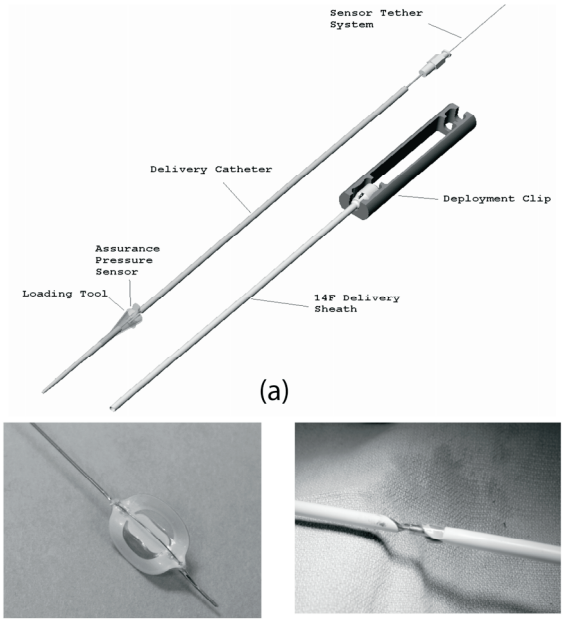

Figure 9 *Sensor delivery system. (a) Schematic of delivery system; (b) sensor on tether; (c) sensor rolled up into sheath prior to implantation*

In order to facilitate folding, additional cut-out features were added to the sensor design in between the planar spiral coils and center pressure-variable capacitor; these are observed in *Figure 5 (a)*. The cut-outs allow for the sensor to be rolled up inside the catheter, illustrated in *Figure 9 (c)*. The delivery procedure introduces the catheter though a cut-down in the femoral artery. The system is advanced into position within the mock aneurysm. The catheter is retracted, exposing the sensor on the tether tube

(a)

(b)

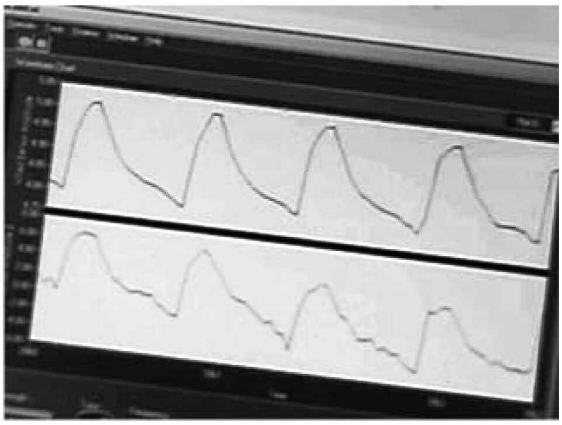

(c)

Figure 10 *Readout telemetry system; (a) system during a measurement while the animal was sedated; (b) antenna on canine during un-sedated measurement; (c) LabVIEW screen-shoot of measurement with the reference signal on the top and wireless pressure sensor on the bottom.*

The sensor is retained on the tether tube until endovascular repair of the aneurysm is completed with a stent graft. Once the sensor is trapped in the space created between the outer surface of the stent graft and the inner surface of the mock aneurysm, the tether wire is pulled, releasing the sensor. The tether tube and delivery catheter are removed, leaving the sensor in the "excluded" portion of the aneurysm sac.

Readout Telemetry

The readout telemetry system consists of switched transmit and receive magnetic loops, a switched RF amplifier and high-sensitivity RF receiver. The system is driven by a microprocessor and phase synchronous oscillator. The system sends a burst of RF energy at the resonant frequency of the devices lasting several microseconds, which is optimized to be long enough to energize the sensor. Soon afterward, the transmit signal is turned off and the receive channel is opened. For a short period of time, based on the sensor quality factor, the sensor will continue to oscillate at the resonant frequency and exponentially decay to zero; this is repeated at the sampling rate of the system. In order to track the sensor real-time frequency response, a phase-locked-loop was implemented. Since the sensors are absolute pressure sensors, a barometric pressure sensor is incorporated into the system to adjust for atmospheric pressure changes in order to report pressure in the aneurysm sac relative to atmospheric pressure. Additional inputs were added to system to be able to readout various catheter based transducers in order to compare to wireless pressure readings. The system is controlled through a LabVIEW software interface, shown in *Figure 10 (c)*. Using this method, devices could be read-out to distances of ≥ 20cm, which was sufficient to achieve measurements in canine models.

Animal Study Results

A total of four devices were implanted into four different animals for a period ranging between 30-60 days. Throughout the study some of the wired reference pressure transducers failed. No failure of the wireless sensors during the study was observed. Also, throughout the study, the telemetry system was improved, which increased the fidelity of the data. The data reported below represents typical results from the four devices. Data was recorded in 60 to 120 second intervals at sampling rates of > 120 Hz, which was sufficient to capture the highest frequency content of interest in the pulse train, illustrated in *Figure 11*. The sensor frequency response to pressure change was determined by pre-implant testing of Fo vs. pressure change in lab testing. At the time of implant, a fluid filled catheter was placed in the aneurysm. The mean (baseline) pressure of this catheter was used as a reference to determine the initial (baseline) mean pressure for the wireless sensor and the wired pressure transducer.

Data was collected beyond 30 days for most of the devices, with pulse pressures ranging between 12 – 37 mmHg and mean pressures ranging from 70 – 120 mmHg. *Figure 12* illustrates the pulse pressure readings over 41 days for both wired and wireless devices. The wireless sensor readings were within the error bars of the reference sensor, indicating low to zero change in response to dynamic pressure changes (pulse pressure). The mean (baseline) frequency drift over the same time is plotted on the secondary axis of *Figure 12*. Over the first six days, the mean frequency drifted by -154 kHz, which is equivalent to an increase in pressure of 28.52 mmHg. Beyond six days the mean frequency continued to drift downward. From the data colleted it is clear that the LCP based sensors are not suitable for applications where an accurate mean pressure reading over time is important. However, this sensor design could be used for long periods of time measuring pulse pressure changes. Improved *in vivo* results are expected from PTFE/ceramic sensors based on results from lab testing.

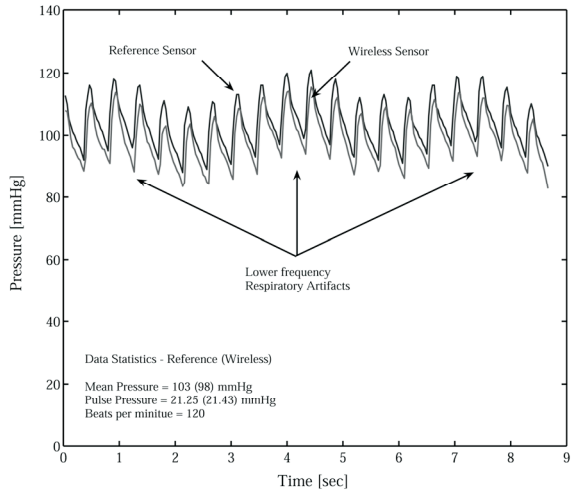

Figure 11 *Continuous pressure waveform of wired and wireless pressure sensor for implanted acute device. Wireless sensor linear sensitivity is -5.76 kHz/mmHg; resonant frequency is 35.675 MHz.*

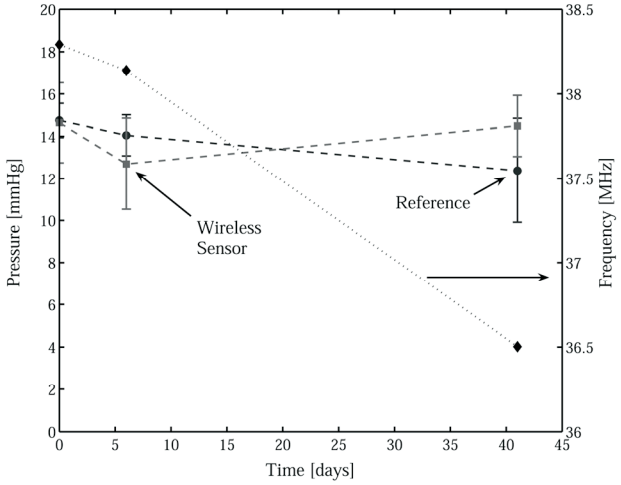

Figure 12 *Pulse pressure vs. time for wired and wireless pressure sensor for acute device (primary axis) and mean resonant frequency vs. time for wireless sensor. Wireless sensor linear sensitivity is -5.4 kHz/mmHg; resonant frequency is 38.293 MHz.*

CONCLUSIONS

The design, modeling, fabrication and characterization for flexible wireless pressure sensors intended for biomedical applications are presented. The devices were fabricated from flexible polymer substrates and optionally-incorporated ceramics, through lamination techniques, in order to implement a passive resonant circuit capable of wireless interrogation. Two sensor designs were presented, one of which is intended for acute use and a second one intended for chronic use. The acute sensor design was implanted, through catheter delivery, into a mock aneurysm in a canine model. Endovascular repair was performed after implantation to exclude the sensor within the aneurysm. Using a telemetry system, measurements of real-time dynamic pressure waveforms were acquired and compared to wired pressure reference transducers. The *in vivo* pulse pressure readings for the wireless acute device showed good correlation to the reference pressure transducer. The acute device drifted in mean (baseline) pressure compared to the reference during the test period. Animal studies on the chronic sensor design have not yet been initiated, but improved baseline drift results are expected based on bench simulated testing. Although neither flexible sensor has yet demonstrated *in-vivo* baseline drift performance of the human-use-approved sensors of [4], both show promise in applications where sensor flexibility is an important factor.

ACKNOWLEDGMENTS

The authors would like gratefully acknowledge Dr. Jay Yadav and Dr. Takao Ohki of the Cleveland Clinic, OH and Montifiore Medical Center, NY, respectively, for their valuable technical input and assistance, as well as the CardioMEMS, Inc. staff, led by CEO David Stern. Also, the authors would like to acknowledge Benjamin King for his assistance in fabrication and characterization, as well as Richard Shafer for his valuable technical discussion.

REFERENCES

[1] R. S. Mackay and B. Jacobson, "Endoradiosonde," *Nature,* vol . 179, pp 1239-1240*,* (June, 1957).

[2] C. C. Collins, "Miniature Passive Pressure Transensor for Implanting in the eye," *IEEE Transactions on Biomedical Engineering*, vol. BME-14, no. 2, (1967).

[3] S. Lizón-Maritinez, R. Giannetti, J. L. Rodrígez-Marrero and B. Tellini, "Design of System for Continuous Intraocular Pressure Monitoring," *IEEE Transaction of Instrumentation and Measurement*, vol. 54, no. 4, (2005).

[4] M. G. Allen, "Micromachined Endovascularly-Implantable Wireless Aneurysm Pressure Sensor: From Concept to Clinic," *Proc. Transducers 2005*, vol 1, pp 275 – 278, (2005).

[5] M. A. Fonseca, J. M. English, M. von Arx, M. G. Allen**,** "High Temperature Characterization of Ceramic Pressure Sensors," *Proc. Transducers 2001*, vol. 1, p 486-489, (2001).

[6] M. A.. Fonseca, J. M. English, M. von Arx, M. G. Allen, "Wireless Micromachined Ceramic Pressure Sensor for High-Temperature Applications," *IEEE/ASME J. Microelectromechanical Systems*, vol. 11, no. 4, p.337-343 (2002)

[7] M. R. Shah, R. P. Phillips and R. A. Normann, "A Study of Printed Spiral Coils for Neuroprosthetic Transcranial Telemetry Applications," *IEEE Transactions on Biomedical Engineering*, vol. 45, no. 7, (1998)

[8] L. A. Sanches et al, "Chronic intraaneurysmal pressure measurement: An experimental method for evaluating the effectiveness of endovascular aortic aneurysm exclusion," *J. Vascular Surgery*, vol. 26, issue 2, pp 222-230, (1997).

[9] P. L. Faries et al, "An Experimental Model for the Acute and Chronic Evaluation of Intra-aneurysmal Pressure," *Valcular Surgery*, pp 290-297, Aug (1997).

[**10]** T. Ohki et al, "Preliminary Results of an Implantable Wireless Aneurysm Pressure Sensor in a Canine Model: Will Surveillance CT Scan Following EVAR Become Obsolete?," *J. Endovascular Therapy*, vol. 10, pp. 1-32, (2003).